

One-dimensional molecular-dynamics simulation of the detonation of nitric oxide

Mark L. Elert

Chemistry Department, U.S. Naval Academy, Annapolis, Maryland 21402

David M. Deaven,* Donald W. Brenner, and C. T. White

Naval Research Laboratory, Washington, D.C. 20375

(Received 22 August 1988)

A series of one-dimensional molecular-dynamics simulations was performed to model the shock-induced initiation of detonation in nitric oxide. Three-body potentials were used to reproduce accurately the energetics of the elementary reactions leading to the formation of the product species, molecular nitrogen and oxygen. The model produces a stable, self-propagating detonation front, without additional parametrization or the introduction of frictional forces. Initiation threshold, reaction-zone widths, product distributions, steady-state detonation-front velocities, and density and temperature profiles resulting from these simulations are presented.

I. INTRODUCTION

Continuum models have been used for many years to predict the behavior of detonating materials. Such models can be quite accurate at the macroscopic scale of interest to designers of explosive devices. However, continuum methods cannot provide information about physical and chemical events taking place at the molecular level during detonation. Experimental information in this regime is also notoriously difficult to obtain, because of the very short time scales and the destructive nature of the processes involved.

Molecular-dynamics simulations provide explicit information about atomic and molecular behavior over short (picosecond to nanosecond) time scales, and are thus ideally suited to the microscale study of detonation and related phenomena. Such methods were first applied to nonreactive shock-wave studies in solids as early as 1966;¹ this work has been extended by several groups since that time.²⁻⁴ The simulation of nonreactive systems is relatively straightforward because atom-atom pair potentials, usually chosen to be of the Lennard-Jones form, suffice to provide a reasonable description of the forces acting in the solid. In contrast, accurate simulation of detonation requires some provision for energy release accompanying chemical reactions in the detonating material. Such processes are inherently many-body problems, since the chemical reactivity of an atom at a given time depends on its current bonding to other nearby atoms in the material.

Molecular-dynamics simulations of detonation have until now relied on the use of a so-called "predissociative potential" to provide energy release during reaction.⁵⁻⁸ In these models a dimer is bound in a metastable state; the molecule can dissociate exothermically after overcoming an energy barrier at intermediate bond length. This method provides an elegant solution to the problem of providing energy release during the simulation while maintaining the simplicity of pair potentials. However, the use of a predissociative pair potential implies that energy release is associated with bond *dissociation*, whereas actual dissociation should be endothermic and *recombina-*

tion (bond formation) should be exothermic. Since these two processes may occur on different time scales, it is possible that simulations based on predissociative pair potentials may cause energy to be deposited unrealistically close to the shock front, resulting in the prediction of incorrect detonation speeds, reaction zone widths, and pressure and temperature profiles.

In this work we demonstrate a method for the incorporation of realistic bond-breaking and bond-forming reactions into a molecular-dynamics model for detonation simulation. We present a one-dimensional model for the condensed phase detonation of nitric oxide according to the reaction



using suitable three-body potentials based on the London, Eyring, Polanyi, and Sato (LEPS) method and demonstrate that the model produces stable detonation behavior with reasonable product distribution, speed, density, and temperature characteristics. Extension of the model to higher dimensions is discussed.

II. MODEL

The one-dimensional system modeled in this work consists of 1024 NO dimers in alternating order, (NOON)₅₁₂. The dimers are arranged in this fashion to permit the three-body chain reactions $\text{N} + \text{NO} \rightarrow \text{N}_2 + \text{O}$ and $\text{O} + \text{ON} \rightarrow \text{O}_2 + \text{N}$ to occur in one dimension. Initially the chain is at complete equilibrium (zero temperature) and at rest. The reaction is initiated by colliding a short segment (NOON)₄ with the larger stationary chain. The initial velocity u_{plate} of the short segment can be varied and this controls the amount of initiation energy provided to the system.

Each atom in the simulation is surrounded on one side by a nitrogen atom and on the other side by oxygen. A minimum requirement for a chemically realistic detonation simulation is that each atom should interact appropriately with its two nearest neighbors. For example, a nitro-

gen atom which has bonded strongly to its nitrogen neighbor to form N_2 should interact via a weak van der Waals potential with its oxygen neighbor, whereas a nitrogen atom which is too far from its nitrogen neighbor for effective bonding should be capable of strong bonding to oxygen.

The three-body potential energy surfaces necessary for implementing reasonable nearest-neighbor interactions were provided by constructing LEPS potentials for the N-N-O and N-O-O systems in the form outlined by Tully.⁹ For each pair of atoms i and j in the three-body system, a 2×2 Hamiltonian matrix H_{ij} is defined as follows:

$$\underline{H}_{ij} = \begin{pmatrix} V_{\text{bond}}(r_{ij}) & 0 \\ 0 & V_{\text{nonbond}}(r_{ij}) \end{pmatrix}, \quad (2)$$

where r_{ij} is the distance between atoms i and j , $V_{\text{bond}}(r_{ij})$ is a diatomic potential function suitable for describing a bound ij dimer, and $V_{\text{nonbond}}(r_{ij})$ represents a weak van der Waals attraction between nonbonded i and j atoms. The ground-state potential energy of the three-body system is the lower eigenvalue of a 2×2 Hamiltonian \underline{H} :

$$\underline{H} = \underline{H}_{12} + \underline{R} \underline{H}_{13} \underline{R}^T + \underline{R}^T \underline{H}_{23} \underline{R}, \quad (3)$$

where \underline{R} is a 2×2 transformation matrix corresponding to a plane rotation of $\pi/3$ radians.

For the NO detonation model under consideration here, bonding and nonbonding pair potentials are required for each of the possible pair interactions N-N, O-O, and N-O. Morse potentials of the form

$$V_{\text{bond}}(r) = D_e (e^{-2\beta(r-r_e)} - 2e^{-\beta(r-r_e)}) \quad (4)$$

with parameters appropriate for the observed ground-state well depths and vibrational frequencies of N_2 , O_2 , and NO were used for the bonding potentials $V_{\text{bond}}(r)$. The role of the nonbonded interaction potentials $V_{\text{nonbond}}(r)$ is to provide a weak, long-range attractive van der Waals force, with potential minima in the range appropriate for molecular N_2 , O_2 , and NO; this helps to stabilize the reactant NO chain. The form of $V_{\text{nonbond}}(r)$ also determines the height of the saddle point separating the two minima on each three-body potential surface. Furthermore, the value of $V_{\text{nonbond}}(r)$ in the van der Waals repulsive core region when r is on the order of a typical bond length (1.1–1.2 Å in this system) must not be so large that it masks the effect of the bonding interaction

TABLE I. Pair potential parameters. D_e , r_e , and β refer to the Morse bonding potential of Eq. (4). The three remaining parameters refer to the nonbonding potential of Eq. (5); ϵ and ρ are well depth and equilibrium separation, respectively, for V_{nonbond} , and are related to the parameters of Eq. (5) by the relations $A = (\epsilon \rho^7)/(6 - \epsilon \rho)$ and $B = [6A/(\epsilon \rho^7)] \exp(\epsilon \rho)$.

Pair type	D_e (eV)	r_e (Å)	β (Å ⁻¹)	α (Å ⁻¹)	ϵ (eV)	ρ (Å)
N-N	9.905	1.098	2.689	0.044	0.259	4.00
O-O	5.214	1.208	2.654	0.047	0.259	4.00
N-O	6.615	1.151	2.743	0.044	0.259	4.00

$V_{\text{bond}}(r)$ in this region of the potential surface. Therefore, a relatively “soft” r^{-6} dependence was chosen for the repulsive core potential, with an exponential form for the attractive component:

$$V_{\text{nonbond}}(r) = A/r^6 - B e^{-ar}. \quad (5)$$

This resembles a standard Buckingham potential except that the signs of the two terms are reversed; however, the numerical values of the parameters used here are substantially different from those generally employed for the Buckingham potential. Other functional forms for $V_{\text{nonbond}}(r)$ could undoubtedly be successfully employed, provided they met the criteria just described.

The three parameters in each of the three $V_{\text{nonbond}}(r)$ functions were chosen so that the saddle points in the resulting three-body LEPS potentials matched the *ab initio* transition-state energies calculated by Walch and Jaffe¹⁰

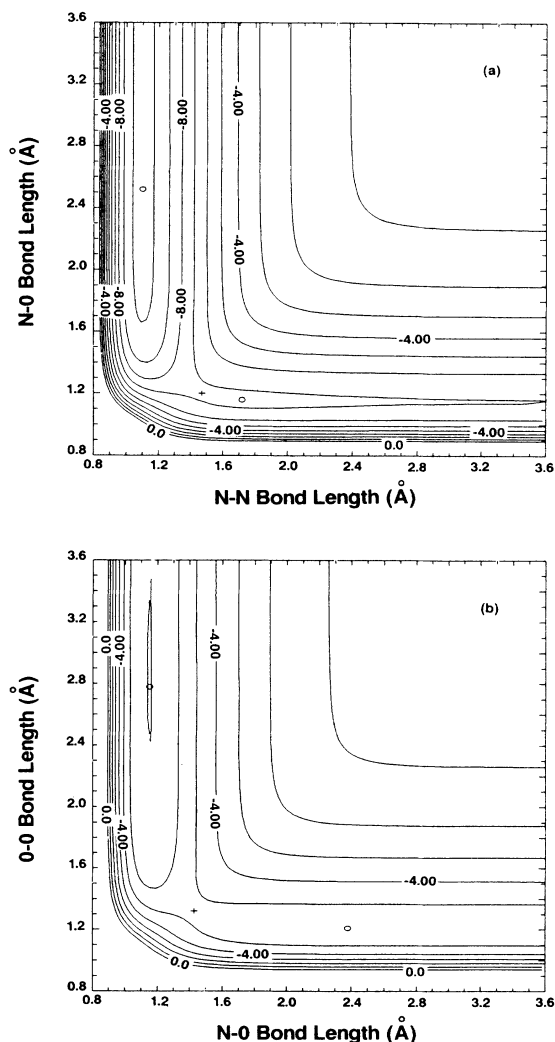


FIG. 1. Contour plots for the LEPS potential surfaces of the linear trimers (a) NNO and (b) NOO. Energies are in eV, bond lengths in Å. Positions of the energy minima (○) and transition states (+) are shown.

for the $N+NO$ and $O+ON$ reactions. (The transition states found by Walch and Jaffe were actually bent configurations, but the same barrier heights are used here to give the best possible one-dimensional model for the actual three-dimensional reactions.) The complete set of potential surface parameters is given in Table I. The resulting N-N-O LEPS potential has an activation barrier of 0.046 eV and an energy change of -3.14 eV for the reaction $N+NO \rightarrow N_2+O$; the N-O-O potential leads to a barrier of 0.455 eV and an energy change of -1.38 eV for the reaction $N+O_2 \rightarrow NO+O$. Equipotential contours for the two possible gas phase trimers are presented in Fig. 1.

We have written the total potential energy of a one-dimensional chain of atoms as a sum of adjacent overlapping LEPS trimer potential energies. With this method, all but the two atoms at each end of the chain are involved in three LEPS interactions: one as the rightmost member of a LEPS trio, one as the central member, and one as the leftmost member. Energies and forces for each atom can be written analytically and evaluated rapidly using this model, making it well suited for numerical simulation studies.

The classical equations of motion for the system were integrated using the Nordseick method¹¹ with provision for a variable time step.¹² The chain of reactant molecules was first quenched to zero degrees Kelvin and equilibrium bond lengths, and a simulation was then initiated by the impact of a short chain segment with a selected velocity u_{plate} . In each case, the total energy of the system was conserved to less than one-half of one percent for simulations of up to 20 psec. A typical 20 psec simulation required approximately 1 h of CPU time on a Cray X-MP/24 supercomputer, or 120 h on a MicroVAX II computer.

III. RESULTS

The time at which the shock or detonation front reaches a particular atomic position can be easily monitored by noting the time when the atom first acquires a given threshold velocity or experiences a threshold force. The average front velocity over any interval may then be determined. Figure 2 shows the shock front velocity versus time for a number of different impact plate velocities u_{plate} . The shocks initiated with impact velocities $u_{plate} \approx 2.5$ km/sec or less are unreactive, and shock velocity decays steadily with time as energy is dissipated via inelastic collisions in the front region. The shocks initiated with impact velocities $u_{plate} \approx 3$ km/sec or more are reactive, and reach a stable detonation front velocity within 5–15 psec of initiation. As Fig. 2 demonstrates, the speed of the detonation front rapidly converges to a value which is independent of the initiation conditions. Experimentally the characteristic detonation velocity for condensed-phase NO is found to be 5.5 km/sec, considerably slower than the 11 km/sec predicted by our model. However, this difference is consistent with the expectation that in a one-dimensional system, with limited degrees of freedom and with all collisions of zero impact parameter and in the direction of detonation propagation, more energy is chan-

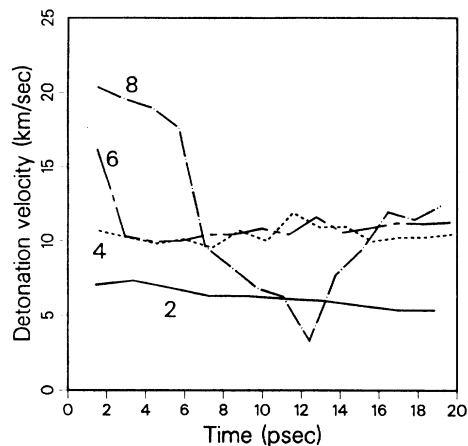


FIG. 2. Detonation front velocity (km/sec) vs time after detonation initiation (psec) for various plate impact speeds. The label for each curve indicates the plate impact speed for that simulation, in km/sec.

neled to the detonation front than in a real three-dimensional system.

Study of the chemical composition of the solid relative to the position of the traveling detonation front shows that the majority of the reactants have been consumed in a very narrow region approximately 20-Å wide behind the front. The exothermic recombination reactions which are responsible for driving the detonation occur over a much wider interval of a few hundred angstroms; this is related to the fact that stable dimers (defined as those for which

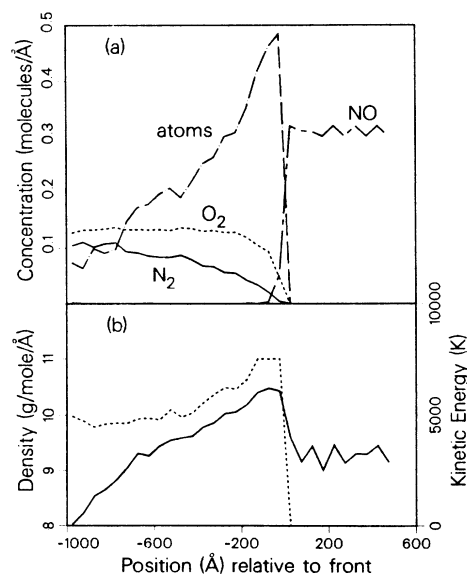


FIG. 3. (a) Concentration (molecules/Å) of each chemical species relative to the front for a simulation with a plate impact velocity of 6 km/sec, averaged over the duration of the 20 psec simulation. (b) Kinetic energy (dashed line) and density (solid line, g/mol/Å) profiles relative to the front for the same simulation.

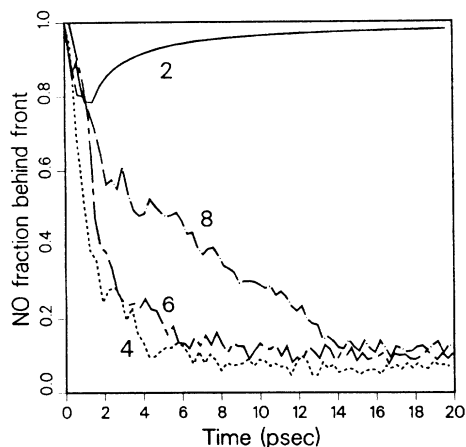


FIG. 4. Fraction of unreacted nitric oxide in the region between the front of the slab and the current position of the detonation front vs time, for various plate impact speeds. The label for each curve indicates the plate impact speed for that simulation, in km/sec.

the sum of the potential and kinetic energies is negative) are unlikely to form in the region immediately behind the front where the average kinetic energy is very high. Figure 3(a) shows the average chemical composition relative to the front for a simulation in which the impact plate velocity was 6 km/sec. Figure 3(b) shows the kinetic energy (expressed in temperature units) and density profiles relative to the front for the same simulation.

At higher-impact plate velocities the detonation is initially overdriven, and the front velocity converges to the steady-state value over a period of several picoseconds. During this interval the reaction efficiency of nitric oxide behind the front is noticeably decreased. (See Fig. 4.) Apparently, at higher atomic velocities the cross sections for the exothermic reactions driving the detonation front decrease, lowering the amount of kinetic energy available and slowing the front velocity until the steady-state value is reached. This mechanism for self-limiting detonation propagation velocity will be explored in more detail elsewhere.¹³

IV. DISCUSSION

This work presents the first molecular-dynamics simulation of a detonating system which incorporates realistic endothermic bond-breaking and exothermic bond-forming reactions. A stable, self-propagating detonation front with a reasonable velocity is achieved using three-body LEPS interaction potentials, without additional parametrization or the introduction of frictional forces. The reaction zone in the stably propagating detonation is found to be quite narrow. Kinetic energy from the exothermic recombination reactions is transmitted to the detonation front via collective atomic motion, allowing the front velocity to be significantly higher than the average atomic velocity in the reaction zone. For overdriven detonations it is found that attainment of the steady detonation velocity characteristic of the reactant material is preceded by a period in which the front velocity oscillates around the steady-state value, suggesting a self-limiting mechanism for achieving and maintaining this value in actual detonating systems.

In higher dimensions the number of neighbors capable of interacting strongly with a given atom will exceed two, and therefore a direct implementation of a LEPS-style three-body interaction potential would not be appropriate. However, the LEPS method has recently been extended¹⁴ to include the simultaneous interaction of more than three species, and other many-body potentials such as the Tersoff potential¹⁵ could also be used. Detonation simulations in two or three dimensions with realistic many-body potentials can be expected to provide quantitative information regarding the initiation and propagation of detonation in condensed phases.

ACKNOWLEDGMENTS

We thank Frank Walker for many helpful discussions, Eric Laing for assistance with the calculations, and the Naval Research Laboratory Research Advisory Committee for a grant of computer time. This work was supported in part by the Office of Naval Research. One of us (M.L.E.) also acknowledges the support of the Naval Research Laboratory-United States Naval Academy Cooperative Program for Scientific Interchange.

*Current address: Department of Physics, University of California, Berkeley, CA 94720.

¹D. H. Tsai and C. W. Beckett, *J. Geophys. Res.* **71**, 2601 (1966).

²A. Paskin and G. J. Dienes, *J. Appl. Phys.* **43**, 1605 (1972).

³D. H. Tsai and R. A. MacDonald, *J. Phys. C* **6**, L171 (1973); *Phys. Rev. B* **14**, 4714 (1976).

⁴A. N. Dremin and V. Yu. Klimenko, *Prog. Astronaut. Aeronaut.* **75**, 253 (1979).

⁵A. M. Karo and J. R. Hardy, *Int. J. Quantum Chem.* **12**, Suppl. 1, 333 (1977).

⁶A. M. Karo, J. R. Hardy, and F. E. Walker, *Acta Astronaut.* **5**, 1041 (1978).

⁷D. H. Tsai and S. F. Trevino, *J. Chem. Phys.* **81**, 5636 (1984).

⁸M. Peyrard, S. Odier, E. Lavenir, and J. M. Schnur, *J. Appl. Phys.* **57**, 2626 (1985); M. Peyrard, S. Odier, E. Oran, J. Boris, and J. Schnur, *Phys. Rev. B* **33**, 2350 (1986).

⁹J. Tully, *J. Chem. Phys.* **73**, 6333 (1980).

¹⁰S. P. Walch and R. L. Jaffe, *J. Chem. Phys.* **86**, 6946 (1987).

¹¹A. Nordseick, *Math. Comp.* **16**, 22 (1962).

¹²C. W. Gear, *Numerical Initial Value Problems in Ordinary Differential Equations* (Prentice-Hall, Englewood Cliffs, NJ, 1971).

¹³D. W. Brenner, M. L. Elert, F. E. Walker, and C. T. White (unpublished).

¹⁴J. H. McCreery and G. Wolken, Jr., *J. Chem. Phys.* **66**, 2316 (1977).

¹⁵J. Tersoff, *Phys. Rev. B* **37**, 6991 (1988).